Ultrasonic Spot Welding of Lightweight Alloys

V.K. Patel[1], S.D. Bhole[1], <u>D.L. Chen</u>[1,*]

[1]Department of Mechanical and Industrial Engineering, Ryerson University, M5B 2K3, Canada
*Corresponding author: dchen@ryerson.ca

Abstract The structural applications of lightweight alloys in the automotive and aerospace industries inevitably involve welding and joining of challenging dissimilar Mg-to-Al and Mg-to-steel while guaranteeing safety and structural integrity. Sound dissimilar lap joints were achieved via ultrasonic spot welding (USW) – an environment-friendly solid-state joining technique. The addition of Sn interlayer during USW effectively blocked the formation of brittle $Al_{12}Mg_{17}$ intermetallic compound in the Mg-to-Al dissimilar joints without interlayer, and led to the presence of a distinctive composite-like Sn and Mg_2Sn eutectic structure in both Mg-to-Al and Mg-to-HSLA (high strength low alloy) steel joints. The lap shear strength of both types of dissimilar joints with a Sn interlayer was significantly higher than that of the corresponding dissimilar joints without interlayer. Failure during the tensile lap shear tests occurred mainly in the mode of cohesive failure in the Mg-to-Al dissimilar joints and in the mode of partial nugget pull-out in the Mg-to-HSLA steel dissimilar joints. In particular, the addition of Sn interlayer resulted in energy saving since the welding energy required to achieve the maximum strength decreased from 1250 J to 1000 J in the Mg-to-Al joints and from 1750 J to 1500 J in the Mg-to-HSLA steel joints.

Keywords Magnesium alloy; Ultrasonic spot welding; Intermetallic compounds; Tin interlayer

1. Introduction

Various industries, especially automotive and aerospace sectors, have a pressing need for structural components that are lighter and stronger, aiming to improve energy efficiencies and reduce anthropogenic environment-damaging emissions and pollution while guaranteeing safety and reliability. Aluminum (Al) and steel have already a wide variety of structural applications in the transportation industry due to their excellent properties, such as good ductility, formability and thermal conductivity. To reduce pollution and save energy [1], ultra-lightweight magnesium (Mg) alloy has increasingly been used in the vehicle fabrication due to its lower density, higher specific strength and stiffness, excellent size stability and acceptable process ability [2]. The structural application of Mg alloys inevitably involves welding and joining of similar Mg-to-Mg alloys and dissimilar Mg-to-Al and Mg-to-steel. In the auto body manufacturing resistance spot welding (RSW) has been a predominant process [3,4]. Since the differences in properties among these metals are large, like melting point, electric conductivity and thermal physical properties, etc., it is fairly challenging to join Mg-to-Al and Mg-to-steel [5,6]. Also, the high-energy consumption and the requirement for frequent electrode maintenance have limited its prevalent application to the Mg-to-Al alloys. Furthermore, in the welding of dissimilar metals a rapid formation of brittle intermetallic compounds (IMCs) occurs, which can seriously degrade the mechanical properties of welded joints [3].

Recently attention has been paid to two solid-state welding processes, namely friction stir spot welding (FSSW) and ultrasonic spot welding (USW), because the liquid phase reaction in the fusion zone during RSW can be avoided. Although FSSW has the potential to produce effective welds between dissimilar materials, the relatively long welding cycle (or time) would be a limiting factor for its widespread adoption in automotive manufacturing [4]. Another solid-state welding technology of USW is able to produce coalescence via a simultaneous application of localized high-frequency vibratory energy and moderate clamping forces [7,8]. In comparison with FSSW, USW has been shown to have a shorter weld cycle (typically <0.4 s) and produce high quality joints that are stronger than FSSW when compared on basis of the same nugget area [9,10]. Besides, the

normal FSSW leaves an exit hole after welding [11]. From the point of view of energy consumption, USW is far more advantageous. For example, welding of aluminum alloys using a USW process consumes only about 0.3 kWh per 1000 joints [4,12], compared to 20 kWh with RSW, and 2 kWh with FSSW [4].

Our previous studies [13] and other investigations [14-17] showed that in the joining of dissimilar Mg-to-Al alloys, the formation of IMCs of $Al_{12}Mg_{17}$ and Al_3Mg_2 seems to be unavoidable. Since the mechanical properties of the welded joints are closely related to the formation of the brittle intermetallic layer [18], it is difficult to obtain a strong joint between Mg and Al alloys. In the study of dissimilar Mg-to-steel joint, Santella *et al.* [19] and Schneider *et al.* [20] reported that Mg and steel do not react with each other and the joint could be easily broken by hand. To improve the mechanical properties of the Mg-to-Al and Mg-to-HSLA steel joints, Chowdhury *et al.* [21] (FSSW) and Xu *et al.* [22] (RSW) have tried to weld Mg-to-Al and Mg-to-HSLA steel joint, respectively, using adhesive placed in-between the faying surface. However, the application of adhesive is a time consuming process. Some researchers have used Zn as an interlayer between Mg and Al alloys [23,24] and Mg and HSLA steel [19,25] for improving the mechanical properties of the dissimilar joints. Others, e.g., Liu *et al.* [26] and Qi and Liu [27] in the tungsten inert gas (TIG) and hybrid laser-TIG welding of Mg-to-Al alloys, respectively, and Liu *et al.* [28] in the hybrid laser-TIG welding of Mg-to-steel, have used Sn as an interlayer and also showed the improvement of the mechanical properties. However, it is unclear how Sn interlayer would affect the microstructure of USWed Mg-to-Al and Mg-to-HSLA steel joints, and if the intermetallic layer would form, and whether Sn interlayer would improve the mechanical properties of the joints. This study was, therefore, aimed to identify the effect of the Sn interlayer on the microstructure and lap shear tensile properties of USWed AZ31B-H24-to-Al5754-O and to-HSLA steel. The selection of Sn in the present study was also based on Mg-Sn, Al-Sn and Fe-Sn binary phase diagrams [29-31], which showed that Sn may interact with Mg and generated IMCs, while Sn might be dissolved into Al and Fe to form solid solution of Sn-Al and Sn-Fe. Furthermore, it was selected on the basis of the findings that Sn improved the wettability of Mg, Al and Fe during the welding process [26,28] and also refined the grain size in the Mg alloy [28,32].

2. Material and Experimental Procedure

In the present study, commercial 2 mm thick sheet of AZ31B-H24 Mg alloy (composition in wt.%: 3Al, 1Zn, 0.6Mn, 0.005Ni, 0.005Fe and balance Mg), 1.5 mm thick sheet of Al5754-O Al alloy (3.42Mg, 0.63Mn, 0.23Sc, 0.22Zr, and balance Al), and 0.8 mm thick sheet of high strength low alloy (HSLA) steel (0.06C, 0.227Si, 0.624Mn, 0.006P, 0.004S, 0.013Ni, 0.041Cr, 0.005Mo, 0.044Cu, 0.039Al, 0.003Ti, 0.021Nb and balance Fe) were selected for the USW. The specimens of 80 mm long and 15 mm wide were sheared, with the faying surfaces ground using 120 emery papers, and then washed using acetone followed by the ethanol and dried before welding. During welding a 50 μm thick pure Sn interlayer was placed in-between the work pieces of Mg/Al and Mg/HSLA steel samples. The welding was conducted with a dual wedge-reed Sonobond-MH2016 HP-USW system. The samples were welded at an energy input ranging from 500 to 2500 J at a constant power setting of 2000 W, an impedance setting of 8 on the machine, and a pressure of 0.414 MPa. Four samples were welded in each welding condition. Two of them were used for microstructural examination and microhardness tests, and the other two were used for the lap shear tensile tests. Cross-sectional samples for scanning electron microscopy (SEM) were polished using diamond paste and MasterPrep. A computerized Buehler microhardness testing machine was used for the micro-indentation hardness tests diagonally across the welded joints using a load of 100 g for 15 s except for the thin IMC interlayer, where a load of 10 g was used for 15 s. The mean value of three indentations along the IMC interlayer was taken for a better accuracy with the low

indentation load of 10 g. To evaluate the mechanical strength of the welded joints and establish the optimal welding conditions, tensile shear tests of the welds were conducted to measure the lap-shear failure load using a fully computerized United testing machine at a constant crosshead speed of 1 mm/min at room temperature in air. In the tensile lap shear testing, restraining shims or spacers were used to minimize the rotation of the joints and maintain the shear loading as long as possible. X-ray diffraction (XRD) was carried out on both matching fracture surfaces of Mg-Al and Mg-HSLA steel sides after tensile shear tests, using CuKα radiation at 45 kV and 40 mA. The diffraction angle (2θ) at which the X-rays hit the samples varied from 20° to 100° with a step size of 0.05° and 2 s in each step.

3. Results and Discussion

3.1 Microstructural evaluation

Microstructural characterization was conducted across the weld line of the samples. Fig. 1(a) and (b) show microstructures at the center of weld nugget of USWed Mg/Al and Mg/HSLA steel joints without a Sn interlayer, respectively. Sound joints were obtained since no large defects were present, such as crack or tunnel type of defects. It is seen from Fig. 1(a) that there was a heterogeneously distributed IMC layer between the Mg and Al alloy sheets. In our previous study [6] of USW of Mg/Al alloys without Sn interlayer, the non-uniform IMC layer had a solidified microstructure containing the brittle phase through the eutectic reaction, liquid→$Al_{12}Mg_{17}$+Mg. In the USWed Mg/HSLA steel joint, as there was no interaction between Mg and Fe, the interface of AZ31B-H24 and HSLA steel was clear without transitional zone, as shown in Fig. 1(b). Due to a large difference of hardness, the sections of Mg alloy and steel were not in the same level in the process of metallographic sample preparation, indicating by white arrows where some hydroxides produced, which will be confirmed by EDS analysis later. Fig. 1(c) and (d) show the welded joints of Mg/Al and Mg/HSLA steel with a Sn interlayer, which could be clearly seen. However, this interlayer was no longer pure Sn interlayer after USW. It became a layer of Sn-Mg_2Sn eutectic structure, which will be identified in the following sections.
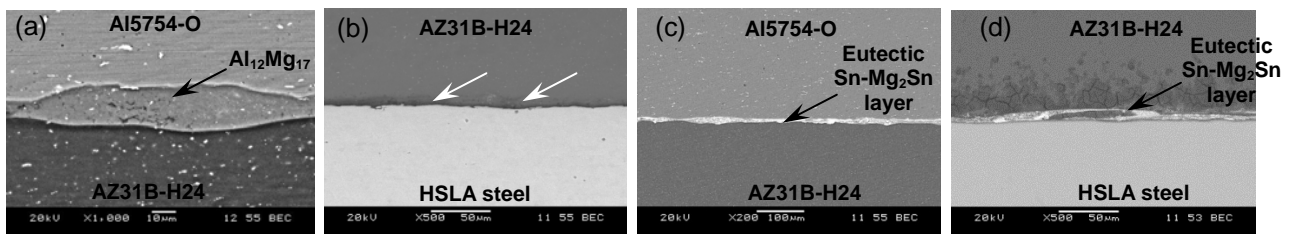
Figure 1. Microstructure of the dissimilar USWed joints made with a welding energy of 1000 J, (a) Mg/Al and (b) Mg/HSLA steel without a Sn interlayer, and (c) Mg/Al and (d) Mg/HSLA steel with a Sn interlayer.

3.2 Energy-dispersive X-ray spectroscopy (EDS) analysis

Fig. 2(a) and (b) show the SEM image at the center of the nugget zone (NZ) of USWed Mg/Al with a Sn interlayer, and its EDS line scan, respectively. The chemical composition (in at.%) at points A and B was 64.4% Mg - 36.4% Al - 1.2% Sn and 63.5% Mg - 21.8% Al - 14.7% Sn, respectively, which suggests that the dark area (A) had less Sn than the white area (B). Fig. 2(c) and (d) show the SEM image at the center of the NZ of USWed Mg/HSLA steel with a Sn interlayer, and its EDS line scan, respectively. The chemical compositions (in at.%) at points C (Fig. 2(c)) was 70.3% Mg-29.7% Sn, suggesting that only Mg and Sn elements were present in the interlayer. The

chemical composition (in at.%) at point D was 62.3% Mg-37.7% O, which suggested the presence of galvanic corrosion product by forming magnesium hydroxide of $Mg(OH)_2$ during the metallographic sample preparation [33,34]. The occurrence of galvanic corrosion was attributed to the large difference between Mg and Fe positioned in the galvanic series. In both Fig. 2(a) and (c), the IMC layer displayed a composite-like eutectic structure at the center of the weld nugget, where the Sn-containing fine white particles were distributed homogeneously or as a network in the interlayer. EDS line scan revealed that the intensity of Al was lower than that of Mg in the NZ of the USWed Mg/Al joint (Fig. 2(b)), and little or no Fe present in the NZ of USWed Mg/HSLA steel (Fig. 2(d)). This was due to the higher solubility of Sn in Mg than Sn in Al and Sn in Fe. Therefore, these results (Fig. 2(d)) in conjunction with the Mg-Sn phase diagram [29] suggested the presence of Mg_2Sn phase, where the eutectic structure consisting of β-Sn (or Mg-Sn solid solution) and Mg_2Sn, which would occur at a temperature of as low as 203°C [29].
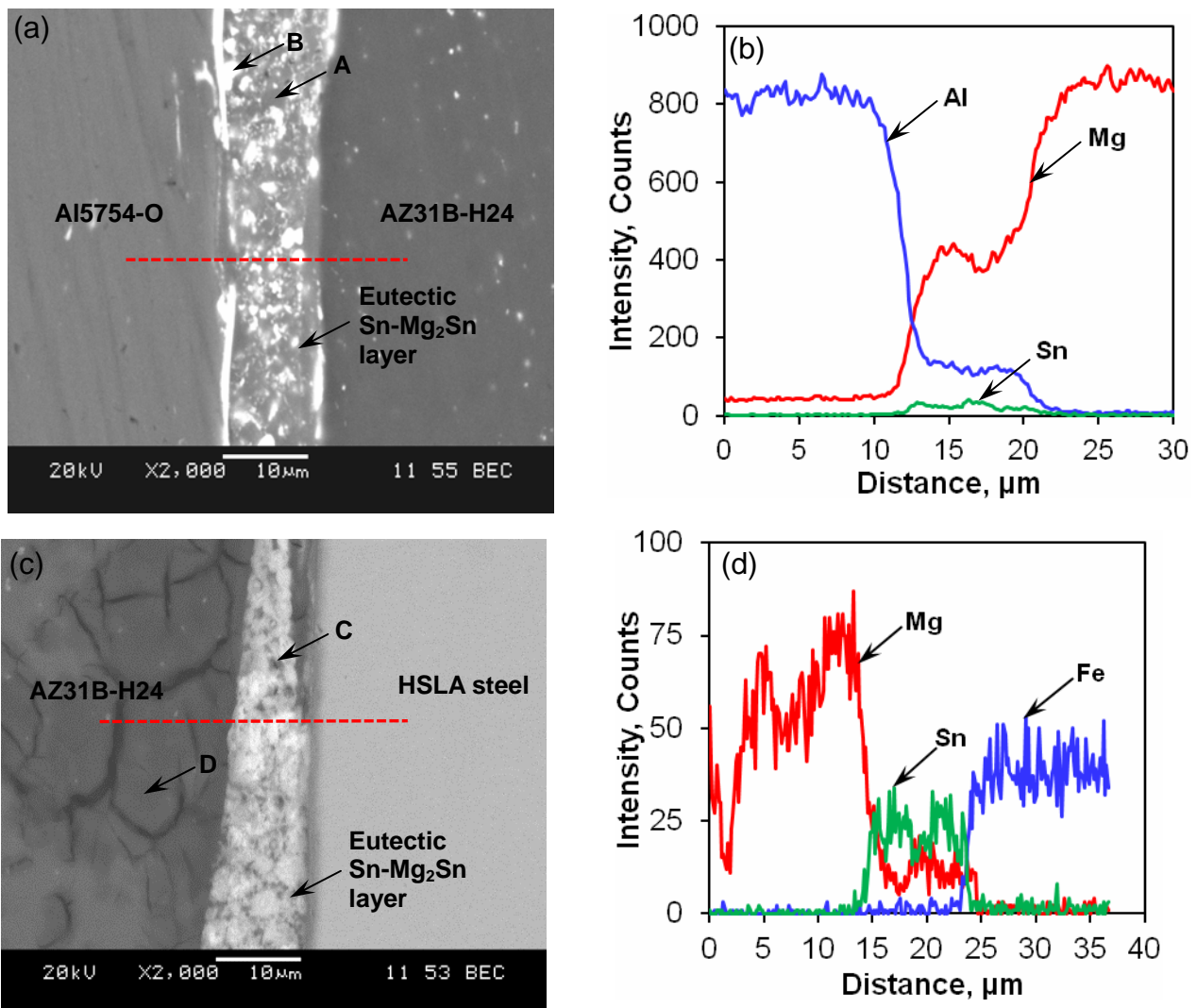
Figure 2. (a) SEM micrograph at the center of NZ of USWed Mg/Al joint and (b) EDS line scan across the interlayer in (a), (c) SEM micrograph at the center of NZ of USWed Mg/HSLA steel joint and (d) EDS line scan across the interlayer in (c) made at a welding energy of 1000 J.

In the USW, the simultaneous application of localized high-frequency vibratory energy and moderate clamping force leads to a fast relative motion and rubbing/friction heat at the interfaces [7,8] between Al-Sn (Mg/Al joint) or Fe-Sn (Mg/HSLA steel joint) and Mg-Sn (in both types of

joints), which would cause a potential melting and coalescence of Sn. In the presence of the Sn interlayer in the USW, Al and Sn in the Mg/Al joint, and Fe and Sn in the Mg/HSLA steel joint combine to form solid solutions, while Mg and Sn combine to form β-Sn and Mg_2Sn IMCs. The Mg_2Sn phase has an antifluorite-type (CaF_2) AB_2 crystal structure with a moderately high melting temperature of 770°C and a lattice parameter of $a = 0.676$ nm [35]. It is apparent that the large Mg_2Sn particles resulted from the eutectic reaction (L $\rightarrow \beta$ Sn + Mg_2Sn) when the temperature reached the eutectic temperature during USW. The addition of Sn to the lap joint was observed to refine the grain size in the fusion zone and the base Mg alloy [28,32] due to the presence of a eutectic Mg_2Sn particles, which restricts the growth of the Mg grains via the Zener pinning pressure (or pinning role). Furthermore, it also improves the wetability of Mg with Al and Fe during the welding process [26,28]. Thus, the surface tension of the liquid was reduced so that more liquid spreads evenly over the surface of the base metal.

3.3 X-ray diffraction analysis

To further verify the above microstructural observations, XRD patterns obtained on both matching fracture surfaces of Mg/Al and Mg/HSLA steel joints after tensile shear tests are shown in Fig. 3(a) and (b), respectively. It is clear that apart from strong peaks of Al on the Al side, Mg on the Mg side and Fe on Fe side, both Sn and Mg_2Sn appeared on both sides of welded joints. It is of interest to note that there was no single peak of $Al_{12}Mg_{17}$ IMCs in the USWed Mg/Al joint. On the other hand, in the Mg/HSLA steel joint Sn worked as an intermediate medium and reacted with both Mg and Fe. Thus, the addition of a Sn interlayer in-between the Mg/Al and Mg/HSLA steel sheets during USW led to the formation of solid solutions of Sn-Al (in the Mg/Al joint), Sn-Fe (in the Mg/HSLA steel joint) and Sn-Mg (in both Mg/Al and Mg/HSLA steel joints), as well as the Sn + Mg_2Sn eutectic structure (in both Mg/Al and Mg/HSLA steel joints). This is in agreement with the SEM observations shown Fig. 2(a) and (c), and EDS analysis shown in Fig. 2(b) and (d).
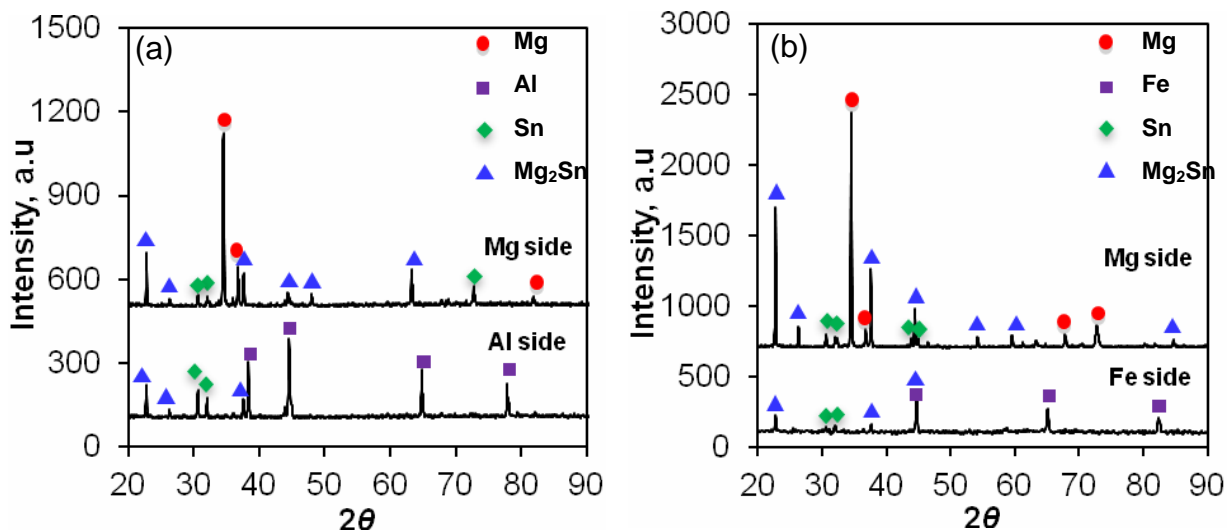
Figure 3. XRD patterns obtained from the matching fracture surfaces of USWed (a) Mg/Al and (b) Mg/HSLA steel joints made at a welding energy of 1000 J.

Furthermore, from our previous studies of USWed Mg/Al joint without any interlayer, lap shear failure occurred predominantly in-between the IMCs of $Al_{12}Mg_{17}$ and Al side [6], i.e., in the mode of "adhesive failure" [36]. However, the presence of Mg_2Sn and Sn eutectic structure on the both sides of the fracture surfaces indicated that the failure occurred mainly through the interlayer. This type of failure is called as the "cohesive failure" which is a desirable failure mode as it assures the use of more strain energy via the weaker part of the joint [36]. Indeed, failure in the USWed

Mg/HSLA steel joint with a Sn interlayer occurred even in the mode of partial nugget pull-out and partial "cohesive failure", giving rise to a higher tensile shear strength which will be seen in the following section.

3.4 Mechanical properties

3.4.1 Microhardness

The hardness profile across the welded joint diagonally is shown in Fig. 4. It is seen that a characteristic hardness profile across the USWed Mg/Al joint was obtained with an average hardness value of about 66 HV on the AZ31B-H24 side and 64 HV on the Al5754-O side, which was basically symmetrical. However, an asymmetrical hardness profile was obtained for the USWed Mg/HSLA steel joint with approximately 61 HV on the AZ31B-H24 side and 145 HV on the HSLA steel side. Interestingly, the hardness value of Mg in the USWed Mg/HSLA steel joint was slightly lower than that of in the USWed Mg/Al joint. This would be associated with the lower thermal conductivity of HSLA steel than Al alloy, which would give rise to a slower cooling rate and higher peak temperature in the welding of Mg/HSLA steel during USW. There were no significant hardness changes in the HAZ in both USWed Mg/Al and Mg/HSLA steel joints, which was in agreement those reported in the literature that USW did not produce a severe HAZ [7,8]. This was related to the relatively low welding temperature that was below the melting points of the welded materials. However, a high hardness value of about 200 HV was detected in the interlayer of both Mg/Al and Mg/HSLA steel joints, as shown in Fig. 4. This was obviously due to the presence of composite-like Mg_2Sn and Sn eutectic structure (Figs 2 and 3), since the hardness value of Mg_2Sn IMCs was higher. This was in agreement with the results reported by other researchers [37,38].
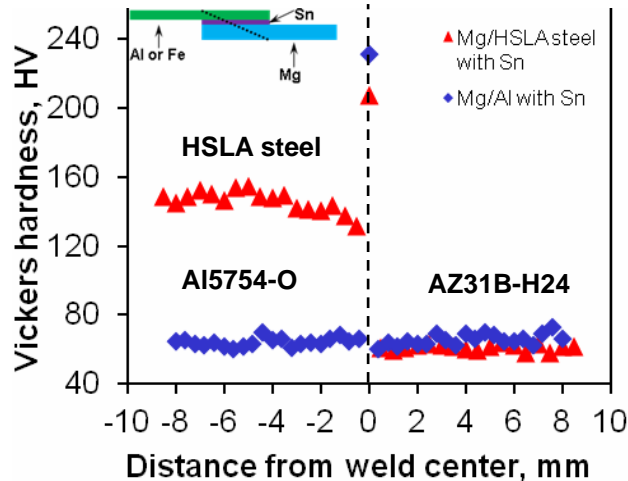
Figure 4. Microhardness profiles across the USWed Mg/Al and Mg/steel joints with a Sn interlayer at a welding energy of 1000 J.

3.4.2 Lap shear tensile strength

As shown in Fig. 5(a), the addition of a Sn interlayer led to an increase in the lap shear strength of both USWed Mg/Al and Mg/HSLA steel dissimilar joints. For example, at a welding energy of 1000 J (Fig. 5(b)), the lap shear strength of USWed Mg/Al and Mg/HSLA steel joints was ~29 MPa and ~45 MPa, respectively, without the addition of a Sn interlayer, and became ~41 MPa and ~54 MPa, respectively, with the addition of a Sn interlayer. This represented an increase of ~55% and ~32% in the lap shear strength for USWed Mg/Al and Mg/HSLA steel joints after a Sn interlayer was added

during USW. Such a significant increase in the lap shear strength was attributed to the formation of solid solutions of Sn-Al, Sn-Fe, Mg-Fe and Mg-Sn, and especially the composite-like eutectic structure of Sn and Mg_2Sn (Figs 2 and 3), instead of the brittle IMCs of $Al_{12}Mg_{17}$ in Mg/Al direct joint [6] and without the interaction of Mg and Fe in Mg/HSLA steel direct joint [28]. In addition, it can be seen from Fig. 5(a) that in the absence of Sn interlayer in the USWed Mg/Al joint, the lap shear strength increased with increasing energy input and reached its maximum at an energy input of 1250 J and then decreased. This was due to the competition between the increasing diffusion bonding arising from higher temperatures at the higher energy inputs and the deteriorating effect of the brittle intermetallic $Al_{12}Mg_{17}$ layer of increasing thicknesses. In the USWed Mg/HSLA steel joint, the lap shear strength increased with increasing energy up to a welding energy of ~1750 J, after which joining was not possible since the tip started to penetrate through the sheets, supposing that it also had the same trend of lap shear strength as that of the USWed Mg/Al joint without Sn interlayer.
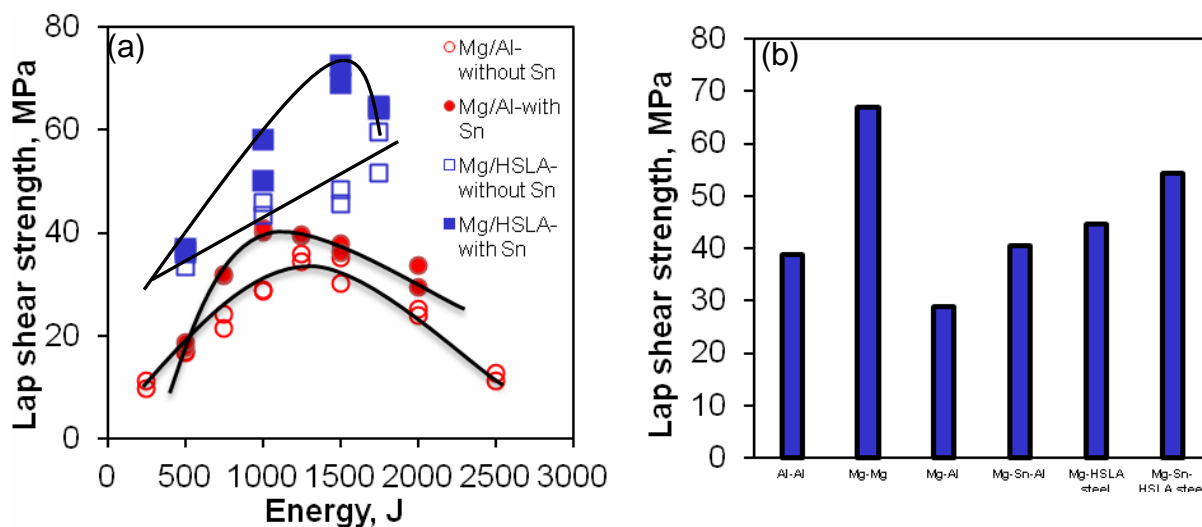
Figure 5. (a) Lap shear strength with and without a Sn interlayer as a function of energy input, (b) comparison of lap shear strength among different welded joints at a welding energy of 1000 J.

In the presence of Sn interlayer, the lap shear strength of both USWed Mg/Al and Mg/HSLA steel dissimilar joints increased initially with increasing welding energy, reached its peak values, followed by a decrease with further increasing welding energy. Such a change occurred due to the fact that at lower energy inputs the temperature was not high enough to soften or melt the Sn interlayer. On the other hand, at higher energy inputs, the specimen was subjected to higher temperatures at larger vibration amplitudes for a longer time, resulting in more Sn interlayer being squeezed out. As summarized in Fig. 5(b), it is seen that the USW of similar joints were fairly effective especially for the Mg/Mg joints with a lap shear strength of 67 MPa. However, the lap shear strength of Al/Al joints made at a welding energy of 1000 J was lower (~39 MPa). The lap shear strength of the USWed Mg/Al dissimilar joint without a Sn interlayer was approximately 25% lower than that of the USWed Al/Al joint and 57% lower than that of the USWed Mg/Mg joint. However, the USWed Mg/Al dissimilar joint with a Sn interlayer had a lap shear strength approximately 5% exceeding that of USWed Al/Al similar joint. The lap shear strength of USWed Mg/HSLA steel dissimilar joint without a Sn interlayer was approximately 33% lower than that of the USWed Mg/Mg similar joint, while with the addition of a Sn interlayer it was about only 19% lower than that of the USWed Mg/Mg similar joint. It is of particular interest to observe that, in addition to enhancing the optimum/maximum lap shear strength in both dissimilar joints, the addition of Sn interlayer also led to an energy saving since the optimal welding energy required to achieve the highest strength decreased from ~1250 J to ~1000 J in the Mg/Al dissimilar joint and

from ~1750 J to ~1500 J in the Mg/HSLA steel dissimilar joint.

4. Conclusions and Remarks

1. The ultrasonic spot welding of AZ31B-H24 Mg alloy to Al5754-O Al alloy and AZ31B-H24 Mg alloy to HSLA steel sheet with a Sn interlayer was successfully performed, with a characteristic composite-like Sn and Mg_2Sn eutectic structure present in the interlayer of both dissimilar joints.

2. The lap shear strength of Mg/Al dissimilar joints with a Sn interlayer was achieved to be significantly higher than that of Mg/Al dissimilar joints without interlayer. This improvement was mainly attributed to the formation of solid solutions of Sn with Mg and Al as well as the composite-like Sn and Mg_2Sn eutectic structure in the interlayer, which effectively prevented the occurrence of brittle $Al_{12}Mg_{17}$ intermetallic compound present in the Mg/Al dissimilar joints without interlayer. The fact that Sn and Mg_2Sn were located on both Al and Mg sides of matching fracture surfaces indicated that the tensile shear failure occurred through the interior of the interlayer in the mode of "cohesive failure".

3. The lap shear strength of Mg/HSLA dissimilar joints with a Sn interlayer was observed to be much higher than that of Mg/HSLA dissimilar joints without interlayer. Sn interlayer actively worked as an intermediate medium to join Mg to Fe by the formation of solid solutions of Sn with Mg and Fe as well as the composite-like Sn and Mg_2Sn eutectic structure in the interlayer.

4. In addition to the beneficial role of enhancing the lap shear strength in both Mg/Al and Mg/HSLA steel dissimilar joints, the addition of Sn interlayer further led to energy saving since the welding energy required to achieve the maximum lap shear strength decreased from 1250 J to 1000 J in the Mg/Al dissimilar joint and from 1750 J to 1500 J in the Mg/HSLA steel dissimilar joint.

5. Further studies are needed to (1) explore other potential interlayers, such as, Zn, Ni, Cu, etc., for further improving the strength of the USWed Mg/Al and Mg/HSLA steel dissimilar joints and (2) evaluate the fatigue and dynamic (or impact) resistance of the dissimilar joints for the safe and reliable applications of the welded lightweight components.

References

[1] J. Murray, D. King, Oil's tipping point has passed. Nature, 481 (2012) 433−435.
[2] T.M. Pollock, Weight loss with magnesium alloys. Science, 328 (2010) 986−987.
[3] R. Qiu, C. Iwamoto, S. Satonaka, Interfacial microstructure and strength of steel/aluminum alloy joints welded by resistance spot welding with cover plate. J Mater Proc Technol, 209 (2009) 4186−4193.

[4]   P.B. Prangnell, F. Haddadi, Y.C. Chen, Ultrasonic spot welding aluminum to steel for automotive applications-microstructure and optimization. Mater Sci Technol, 27 (2011) 617−624.

[5]   X. Qi, G. Song, Interfacial structure of the joints between magnesium alloy and mild steel with nickel as interlayer by hybrid laser-TIG welding. Mater Des, 31 (2010) 605–609.

[6]   V.K. Patel, S.D. Bhole, D.L. Chen, Microstructure and mechanical properties of dissimilar welded Mg-Al joints by ultrasonic spot welding technique. Sci Technol Weld Join, 17 (2012) 202−206.

[7]   R. Jahn, R. Cooper, D. Wilkosz, The effect of anvil geometry and welding energy of microstructures in ultrasonic spot welds of AA6111-T4. Metall Mater Trans A, 38 (2007) 570−583.

[8]   E. Hetrick, R. Jahn, L. Reatherford, J. Skogsmo, S. Ward, D. Wilkosz, J. Devine, K. Graff, R. Gehrin, Ultrasonic spot welding: A new tool for aluminum joining. Weld J, 84 (2005) 26−30.

[9]   P.B. Prangnell, D. Bakavos, Novel approaches to friction spot welding thin aluminium automotive sheet. Mater Sci Forum, 638-642 (2010) 1237−1242.

[10] V.K. Patel, S.D. Bhole, D.L. Chen, Influence of ultrasonic spot welding on microstructure in a magnesium alloy. Scripta Mater, 65 (2011) 911–914.

[11] S.H. Chowdhury, D.L. Chen, S.D. Bhole, X. Cao and P. Wanjara, Lap shear strength and fatigue life of friction stir spot welded AZ31 magnesium and 5754 aluminum alloys. Mater Sci Eng A, 556 (2012) 500–509

[12] D. Bakavos and P.B Prangnell, Mechanisms of joint and microstructure formation in high power ultrasonic spot welding 6111 aluminum automotive sheet. Mater Sci Eng A, 527 (2010) 6320−6334.

[13] V.K. Patel, S.D. Bhole, D.L. Chen, Improving weld strength of magnesium to aluminum dissimilar joints via tin interlayer during ultrasonic spot welding. Sci Technol Weld Join, 17 (2012) 342–347.

[14] D. Choi , B. Ahn ,C. Lee , Y. Yeon, K. Song, S. Jung, Formation of intermetallic compounds in Al and Mg alloy interface during friction stir spot welding. Intermetallics, 19 (2011) 125–130.

[15] Y.C. Chen and K. Nakata, Friction stir lap joining aluminum and magnesium alloys. Scripta Mater, 58 (2008) 433–436.

[16] Y.S. Sato, A. Shiota, H. Kokawa, K. Okamoto, Q. Yang, C. Kim, Effect of interfacial microstructure on lap shear strength of friction stir spot weld of aluminum alloy to magnesium alloy, Sci Tech Weld Join, 15 (2010) 319–324.

[17] A. Panteli, Y. Chen, D. Strong, X. Zhang, P. Prangnell, Optimization of aluminum to magnesium ultrasonic spot welding. JOM, 64 (2012) 414–420.

[18] L. Liu, X. Qi, Strengthening effect of nickel and copper interlayers on hybrid laser-TIG welded joints between magnesium alloy and mild steel. Mater Des, 31 (2010) 3960–3963.

[19] M. Santella, T. Franklin, J. Pan, T.Y. Pan, E. Brown, Ultrasonic spot welding of AZ31B to galvanized mild steel. SAE Inter, 3 (2010) 652–657.

[20] C. Schneider, T. Weinberger, J. Inoue, T. Koseki, N. Enzinger, Characterization of interface of steel/magnesium FSW. Sci Tech Weld Join, 16 (2011) 100–106.

[21] S.H. Chowdhury, D.L. Chen, S.D. Bhole, X. Cao and P. Wanjara, Lap shear strength and fatigue behavior of friction stir spot welded dissimilar magnesium-to-aluminum joints with adhesive. Mater Sci Eng A, 562 (2013) 53–60.

[22] W. Xu, D.L. Chen, L. Liu, H. Mori, Y. Zhou, Microstructure and mechanical properties of weld-bonded and resistance spot welded magnesium-to-steel dissimilar joints. Mater Sci Eng A, 537 (2012) 11–24.

[23] L.M. Zhao, Z.D. Zhang, Effect of Zn interlayer on interface microstructure and strength of diffusion-bonded Mg-Al joints. Scripta Mater, 58 (2008) 283–286.

[24] H.T. Zhang, J.Q. Song, Microstructural evolution of aluminum/magnesium lap joints welded using MIG process with zinc foil as an interlayer. Mater Lett, 65 (2011) 3292–3294.

[25] S. Jana, Y. Hovanski, G.J Grant, Friction stir lap welding of Magnesium alloys to steel: A preliminary investigation. Metall Mater Trans A, 41 (2010) 3173–3182.

[26] X.J. Liu, R.S. Huang, H.Y. Wang, S.H. Liu, Improvement of TIG lap weldability of dissimilar metals of Al and Mg. Sci Tech Weld Join, 12 (2007) 258–260.

[27] X.D. Qi, L. Liu, Fusion welding of Fe-added lap joints between AZ31B magnesium alloy and 6061 aluminum alloy by hybrid laser-tungsten inert gas welding technique. Mater Des, 33 (2012) 436–443

[28] L. Liu, X. Qi, Z. Wu, Microstructural characteristics of lap joint between magnesium alloy and mild steel with and without the addition of Sn element, Mater Lett 64 (2010) 89–92.

[29] A.A Nayeb-Hashemi, J.B. Clark, The Mg-Sn (magnesium-tin) system. Bulletin of alloy phase diagram, 5 (1984) 466–475.

[30] A.J. McAlister, D.J Kahan, Binary alloy phase diagrams, in: T. B. Massalski (Eds.) Al–Sn (Aluminum–Tin), 2nd Eds, Vol. 1, ASM International, Materials Park, OH, 1990, pp. 215–216.

[31] M. Singh, S. Bhan, Contribution to the Fe-Sn system. J Mater Sci Lett, 5 (1986) 733–735.

[32] A.A. Luo, P. Fu, L. Peng, X. Kang, Z. Li and T. Zhu, Solidification microstructure and mechanical properties of cast magnesium-aluminum-tin alloys. Metall Mater Trans A, 43 (2012) 360–368.

[33] C. Liu, D.L. Chen, S. Bhole, X. Cao and M. Jahazi, Polishing-assisted galvanic corrosion in the dissimilar friction stir welded joint of AZ31 magnesium alloy to 2024 aluminum alloy. Mater Charact, 60 (2009) 370–376.

[34] G.L. Song, B. Johannesson, S. Hapugoda, D. StJohn, Galvanic corrosion of magnesium alloy AZ91D in contact with an aluminum alloy, steel and zinc. Corr Sci, 46 (2004) 955–977.

[35] E. Doernberg, A. Kozlov, R. Schmid-Fetzer, Experimental investigation and thermodynamic calculation of Mg-Al-Sn phase equilibria and solidification microstructures. J Phase Equilib Diffu, 28 (2007) 523–535.

[36] W. Xu, L. Liu, Y. Zhou, H. Mori, D.L. Chen, Tensile and fatigue properties of weld-bonded and adhesive-bonded magnesium alloy joints, Mater Sci Eng A, 563 (2013) 125–132.

[37] B.H. Kim, J.J. Jeon, K.C. Park, B.G. Park, Y.H. Park, I.M. Park, Microstructural characterization and mechanical properties of Mg-xSn-Al-Zn alloys. Arch Mater Sci Eng, 30 (2008) 93–96.

[38] V. Kevorkijan, S.D Skapin, Studies of Mg$_2$Sn based composite. MJoM, 16 (2010) 47–61.